Theoretical Study of the Acid-catalysed Friedel–Crafts Reaction between CH_3F and CH_4

Vicenç Branchadell, Antonio Oliva, and Juan Bertrán *
Departament de Química, Universitat Autònoma de Barcelona, 08193 Bellaterra, Spain

The Friedel–Crafts alkylation reaction between methyl fluoride and methane, catalysed by H^+, has been studied by means of SCF and MP2 calculations, using the 3-21G and 6-31G* basis sets. It has been found that the catalyst notably diminishes the potential-energy barrier of the process by increasing the electrophilic character of the alkylating agent. Different mechanisms of catalytic action have been discussed. It has been found that the formation of a $C_2H_7^+$ carbocation plays an important role in the mechanism of the catalysed reaction, in good agreement with experimental predictions.

The Friedel–Crafts reaction is one of the most characteristic examples of the catalytic process in organic chemistry.[1] Of these reactions, the alkylation of aliphatic and aromatic compounds by alkyl halides in the presence of acid catalysts has been the subject of great interest.[2–6]

In particular, Olah *et al.* have studied the alkylation of methane by methyl fluoride in the presence of SbF_5 and detected the formation of ethane and a considerable amount of secondary products.[5] In order to interpret these results, they have proposed a mechanism in which methyl fluoride and SbF_5 form a highly polarized donor–acceptor complex capable of effecting attack on methane. The presence of such complexes has been experimentally detected in several cases, the degree of their polarization varying from one case to another.[4,7–10]

Few theoretical studies have been devoted to the Friedel–Crafts reaction.[11–15] Most of them have only considered the formation of donor–acceptor complexes between several alkyl halides and BF_3[11,14] and H^+.[13] In a previous paper[15] we studied the reaction between methane and hydrogen fluoride, catalysed by H^+ and BF_3, as a simple model of a Friedel–Crafts reaction. The calculations were carried out at the SCF level with the 3-21G basis set. The results obtained showed that the formation of a complex with the catalyst increases the electrophilic character of hydrogen fluoride and, as a direct consequence, the potential-energy barrier of the electrophilic attack step is drastically diminished.

The purpose of this paper is to conduct a more complete study of this type of process. For this reason we have chosen a more realistic reaction model and used a basis set of better quality. We have studied the reaction between methane and methyl fluoride catalysed by H^+. This will permit us to obtain a more thorough understanding of Friedel–Crafts alkylation reactions in the presence of acid catalysts.

Method of Calculation.—*ab initio* SCF and post-SCF calculations have been carried out by means of the GAUSSIAN-86 system of programs[16] using the 3-21G[17] and 6-31G*[18] basis sets. Electron correlation has been included using second order Møller–Plesset theory, MP2,[19] with the 6-31G* basis set. All stationary points have been fully optimized at the SCF level with both basis sets using the Schlegel algorithm.[20] The 3-21G basis set has been used in a preliminary exploration of the potential-energy hypersurface. Transition states and energy minima have been characterized through analytical calculation of the force constants matrix.[21] These 3-21G structures have been taken as starting points in the localization of the stationary points of the 6-31G* potential energy hypersurface. Finally, single point MP2 calculations have been performed for these structures.

Table 1. Energy relative to reactants[a] for the stationary points of the reaction between methane and methyl fluoride.

Stationary point	3-21G	6-31G*	MP2/6-31G*[b]
Reactants	0.0	0.0	0.0
Intermediate	−3.4	−0.9	−1.7
Transition state	117.9	122.3	109.1
Products	2.9	−1.2	−5.4

[a] kcal mol^{-1}. [b] At the 6-31G* geometry.

Results and Discussion

Since we are interested in analysing the role played by the catalyst in the alkylation reaction we will first study the mechanism of the uncatalysed reaction. The mechanism of the catalysed reaction will be discussed later. It is to be noted that the geometries of the 3-21G stationary points are in all cases similar to those obtained with the 6-31G* basis set. For this reason we will only present the 6-31G* geometries and we will use the 3-21G results only to compare the relative energies.

Uncatalysed Reaction.—The reaction between methane and methyl fluoride leads to the formation of ethane and hydrogen fluoride. Table 1 presents the energies referred to reactants for the stationary points localized along the reaction co-ordinate.

The reaction is basically a one step process with prior formation of a complex between the reactants. The 6-31G* structure of this complex is depicted in Figure 1(*a*). It corresponds to a weak hydrogen-bonded complex, with a charge transfer to methane of 0.009 au.†

The potential barrier of the process is very high at all levels of calculation, so that the uncatalysed reaction is a very unfavourable process. The structure of the 6-31G* transition state, which involves a planar four-membered ring, is shown in Figure 1(*b*).

As regards the thermicity of the reaction, the results are different depending on the level of calculation considered. The reaction is slightly endothermic at the 3-21G level, in contrast to the 6-31G* and MP2/6-31G* calculations. The value of the

† The atomic unit (au) of charge, *e*, is $\approx 1.6022 \times 10^{-19}$ C.

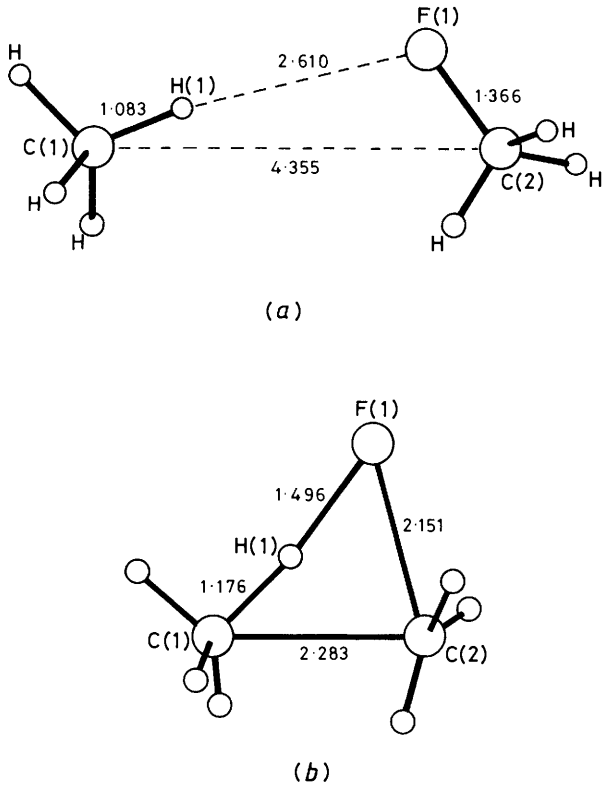

Figure 1. Structures of the 6-31G* stationary points of the reaction between methyl fluoride and methane. (*a*) $CH_3F{\cdot}CH_4$ complex and (*b*) transition state. Interatomic distances in Å.

Table 2. Formal decomposition of the energy barrier[a] of the reaction between methane and methyl fluoride.

	3-21G	6-31G*	MP2/6-31G*[b]
E_{dis} (CH_4)	21.9	7.8	6.9
E_{dis} (CH_3F)	87.7	108.2	96.8
E_{int}	8.3	6.2	5.4

[a] E_{dis} and E_{int} are the distortion energy and interaction energy terms, respectively. All values are in kcal mol^{-1}. [b] At the 6-31G* geometry.

reaction energy is in all cases very small, so that the reaction can be considered almost athermic.

The alkylation reaction involves the formation of the C(1)–C(2) and H(1)–F(1) bonds, while the C(1)–H(1) and C(2)–F(1) bonds are broken. At the transition state the interatomic distance between C(1) and C(2) is still notably greater than that corresponding to ethane (1.528 Å). In the same way, the H(1)–F(1) bond has not reached an important degree of formation. Furthermore, the C(2)–F(1) bond has been broken to a greater extent than the C(1)–H(1) bond. These facts, and the great value of the energy barrier seem to indicate that the stabilization due to the formation of the two new bonds is too small to compensate for the steric repulsion between both reactant molecules and the destabilization caused by the partial cleavage of the C(1)–H(1) and C(2)–F(1) bonds.

In order to confirm the validity of this argument we have performed a decomposition of the energy barrier of the reaction in three terms. The first and the second, the distortion energy terms, are the energies necessary to distort the methane and the methyl fluoride molecules, respectively, from their equilibrium geometry to the geometry they adopt in the transition state. The third term, the interaction energy, is calculated as the difference between the energy of the transition state and the energies of the distorted CH_4 and CH_3F molecules. The results of this energy decomposition are presented in Table 2.

One can observe that the distortion energy terms are both destabilizing at all levels of calculation, especially that corresponding to methyl fluoride. This is basically due to the lengthening of the C(2)–F(1) bond, which has reached an important degree of cleavage at the transition state (see Figure 1). The interaction energy, which takes into account the bonding and non-bonding interactions between the distorted fragments is, in this case, also destabilizing. Therefore, the degree of bond formation is not enough to compensate for the repulsive interaction between both fragments. These results clearly show that the cleavage of the C(2)–F(1) bond is mainly responsible for the great energy barrier.

The Mulliken population analysis of the 6-31G* transition state shows a great polarization of the C(2)–F(1) bond, since the net charges over the CH_3 and F fragments are 0.577 and −0.718 au, respectively, in contrast with 0.404 and −0.404 au in the methyl fluoride equilibrium geometry. Therefore, it is easy to understand the great destabilization of the system, since the dissociation of CH_3F into CH_3^+ and F^- is very unfavourable (284.6 kcal mol^{-1} at the 6-31G* level).†

Catalysed Reaction.—As we have already discussed the first step of the catalysed reaction involves the formation of a complex between the catalyst and the electrophilic reactant. For this reason we will first consider the formation of this complex.

Methyl fluoride–catalyst complex. Figure 2 presents the structures of methyl fluoride and its complex with H^+. It can be observed that protonation leads to an important lengthening of the C–F bond. This is accompanied by a great increase in the net charge over the CH_3 fragment, from 0.404 au in methyl fluoride to 0.802 au in CH_3FH^+. These facts clearly show that the main role played by the catalyst in a Friedel–Crafts reaction is to magnify the electrophilic character of the alkylating agent.

The protonation energy of methyl fluoride is −147.0 kcal mol^{-1} with the 3-21G basis set and −151.4 kcal mol^{-1} with the 6-31G* basis set. These values are in very good agreement with the experimental proton affinity, 151 kcal mol^{-1}.[22]

Electrophilic attack. Olah *et al.*[5] have proposed that the alkylation of methane with methyl fluoride in the presence of SbF_5 takes place through the formation of $C_2H_7^+$. One can consider two different ways in which this carbocation could be formed. The first is the dissociation of CH_3FH^+ into CH_3^+ and HF, followed by a reaction between the methyl cation and methane (Scheme 1).

In the second mechanism the electrophilic agent is CH_3FH^+ itself and the reaction with methane leads to the formation of a $C_2H_7^+{\cdot}FH$ complex. This complex can then dissociate into $C_2H_7^+$ and HF or, through an intramolecular proton transfer, form a $C_2H_6{\cdot}H_2F^+$ complex which dissociates into ethane and protonated hydrogen fluoride (Scheme 2).

In this section we will study these different mechanisms in order to discuss which seems to be the most efficient in the alkylation reaction.

Let us first analyse the mechanism represented in Scheme 1. In Table 3 we present the reaction energies of the first two steps, *i.e.* the dissociation of CH_3FH^+ and the formation of $C_2H_7^+$. The deprotonation of this carbocation will be considered later. The dissociation of CH_3FH^+ into CH_3^+ and HF is clearly an endothermic process, the computed energies being in very good agreement with the experimental results. However, this dissociation energy is much lower than that corresponding to the dissociation of CH_3F into CH_3^+ and F^- (see above). This result

† 1 cal = 4.184 J.

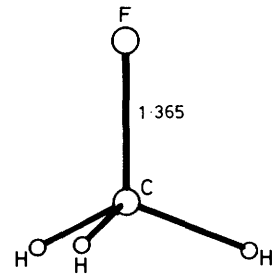

(*a*)

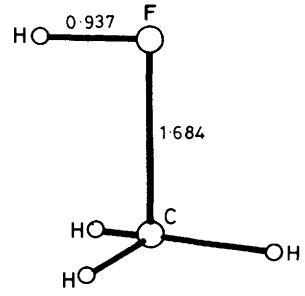

(*b*)

Figure 2. Structures of methyl fluoride (*a*) and protonated methyl fluoride (*b*) obtained with the 6-31G* basis set. Interatomic distances in Å.

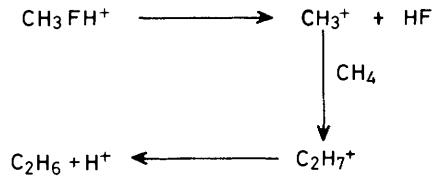

Scheme 1.

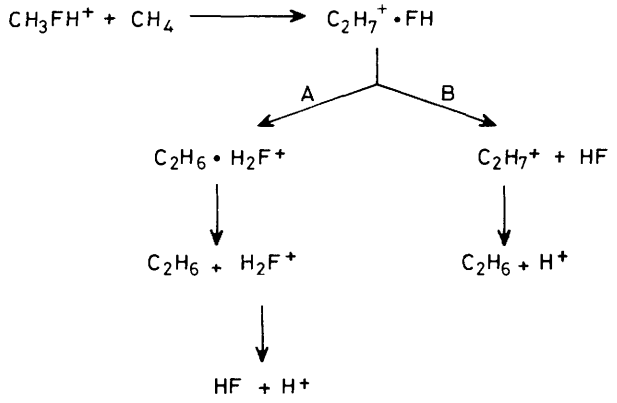

Scheme 2.

confirms that the catalyst increases the electrophilic character of CH_3F, since it facilitates the cleavage of the C–F bond and the formation of CH_3^+.

The reaction between CH_3^+ and methane leading to the C–C bridged isomer[24] of $C_2H_7^+$ is an exothermic process, as shown in Table 3. The reaction energy is underestimated at the SCF level, but the MP2/6-31G* result is in very good agreement with the experimental value. This fact has already been reported by

Table 3. Reaction energies[a] for the dissociation of CH_3FH^+ (ΔE_1) and the formation of $C_2H_7^+$ (ΔE_2).

	ΔE_1	ΔE_2
3-21G	29.3	−22.7
6-31G*	26.6	−18.5
MP2/6-31G*[b]	33.7	−35.9
Experimental	36[c]	−36[d]

[a] kcal mol^{-1}. [b] At the 6-31G* geometries. [c] Ref. 22. [d] Ref. 23.

Table 4. Energies relative to reactants[a] for the reaction between CH_3FH^+ and methane leading to the formation of a $C_2H_7^+$·FH intermediate.

Stationary point	3-21G	6-31G*	MP2/6-31G*[b]
$CH_3FH^+ + CH_4$	0.0	0.0	0.0
CH_3FH^+·CH_4	−6.4	−4.9	−14.3
Transition state	16.7	9.9	13.1
$C_2H_7^+$·FH	2.9	−2.7	−16.0

[a] kcal mol^{-1}. [b] At the 6-31G* geometry.

Ragavachari *et al.*[24] using the 6-31G** basis set. According to Hiraoka and Kebarle[23] the reaction takes place without any energy barrier. For this reason the rate of formation of $C_2H_7^+$ is controlled by the dissociation of CH_3FH^+.

In the mechanism represented in Scheme 2 the first step leads to the formation of a $C_2H_7^+$·FH intermediate. The energies relative to reactants corresponding to the stationary points of the potential-energy hypersurface of this process are presented in Table 4, and the structures of the 6-31G* stationary points are represented in Figure 3.

The formation of the $C_2H_7^+$·FH intermediate involves the prior formation of a hydrogen-bonded complex between CH_3FH^+ and CH_4 [Figure 3(*a*)]. This complex is more stable than that corresponding to the uncatalysed reaction (Table 1).

The relative energy of $C_2H_7^+$·FH with respect to CH_3FH^+ and methane is very small at the SCF level, positive with the 3-21G basis set and negative in the 6-31G* results, this exothermicity being noticeably increased when electron correlation is included. The Mulliken population analysis of the $C_2H_7^+$·FH intermediate shows that the positive charge is located on the C_2H_7 fragment, 0.973 au at the 6-31G* level. Therefore, the formation of this complex can be formally considered as a CH_3^+ transfer from CH_3FH^+ to methane.

The interatomic distances presented in Figure 3 show that the C(2)–F(1) bond at the transition state has been broken to a greater extent than in the case of the uncatalysed reaction [Figure 1(*b*)]. On the other hand, the methane molecule has scarcely been distorted and the C(2)–H(1) bond has still not begun to be formed. These facts show that, although the C(2)–F(1) bond is almost broken at the transition state, the CH_3^+ transfer to methane has not yet been produced. The Mulliken population analysis confirms the existence of a CH_3^+ fragment with net charge 0.949 au at the 6-31G* level.

As indicated in Scheme 2, once the $C_2H_7^+$·FH intermediate has been formed two alternative pathways, A and B, can lead to the reaction products, ethane and hydrogen fluoride. We will first discuss pathway A, which involves an intramolecular proton transfer from the $C_2H_7^+$ fragment to the HF fragment. Table 5 presents the energies relative to the $C_2H_7^+$·FH intermediate for the stationary points localized along the reaction co-ordinate. It can be observed that at all levels of calculation the process is clearly endothermic. At the SCF level a transition state and an intermediate have been found with both basis sets. However, the real existence of these stationary

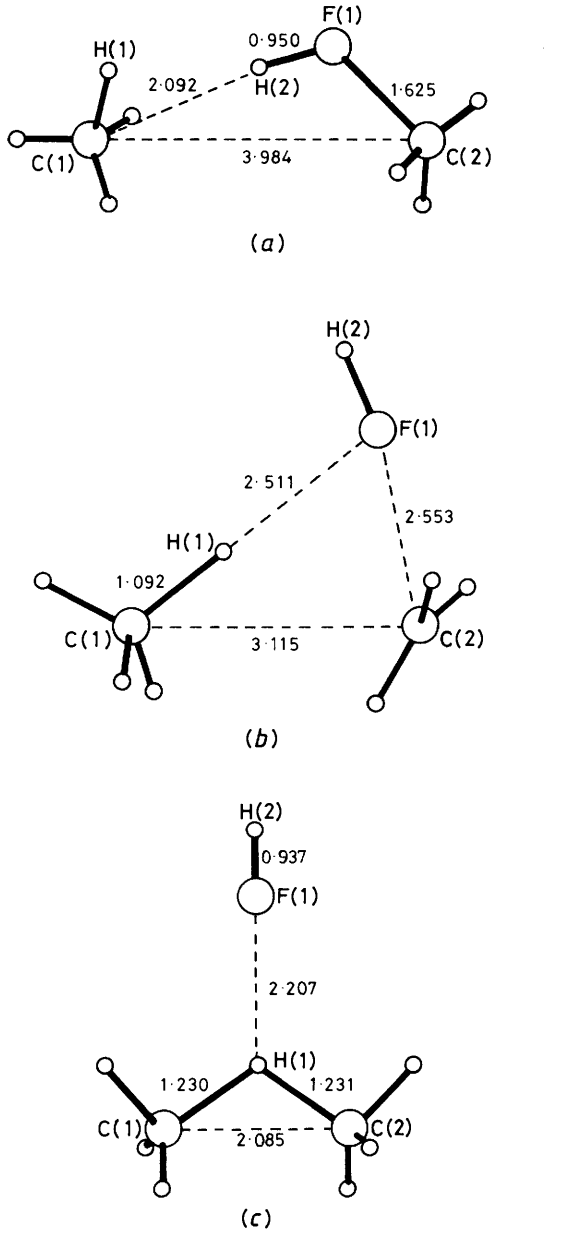

Figure 3. Structures of the 6-31G* stationary points of the reaction between protonated methyl fluoride and methane. (*a*) $CH_3FH^+ \cdot CH_4$ complex; (*b*) transition state; and (*c*) $C_2H_7^+ \cdot FH$ complex. Interatomic distances in Å.

Table 5. Energy relative to the $C_2H_7^+ \cdot FH$ intermediate[a] for the intermolecular proton transfer leading to the formation of ethane and H_2F^+.

Stationary point	3-21G	6-31G*	MP2/6-31G*[b]
$C_2H_7^+ \cdot FH$	0.0	0.0	0.0
Transition state	13.71	18.73	8.8
$C_2H_6 \cdot H_2F^+$	13.70	18.70	9.4
$C_2H_6 + H_2F^+$	28.0	30.6	27.4

[a] kcal mol^{-1}. [b] At the 6-31G* geometry.

points can be questioned since the intermediate is situated in a well of very little depth (0.01 kcal mol^{-1} with the 3-21G basis set and 0.03 kcal mol^{-1} with the 6-31G* set). In fact, the single point

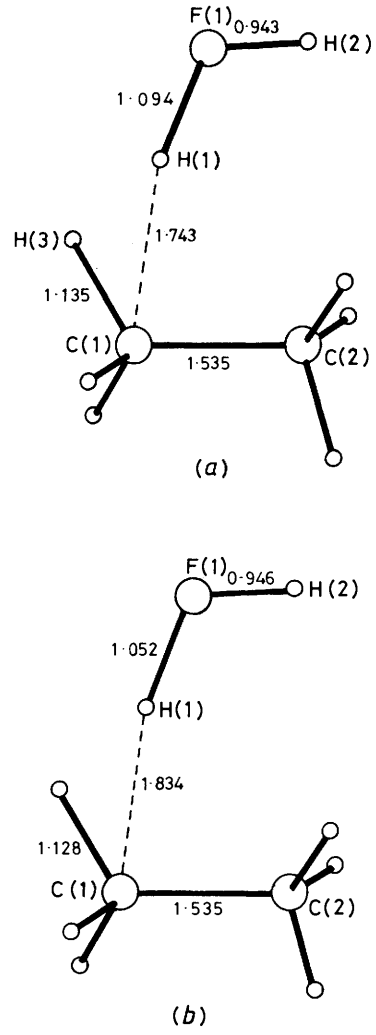

Figure 4. Structures of the 6-31G* transition state (*a*) and intermediate (*b*) of the intramolecular proton-transfer process from the $C_2H_7^+ \cdot FH$ complex to $C_2H_6 + H_2F^+$. Interatomic distances in Å.

Table 6. Calculated and experimental proton affinites of hydrogen fluoride, ethane and methane.

	3-21G	6-31G*	Experimental
HF	131.9	122.3	112[b]
C_2H_6	143.3	142.1	146.9[c]
CH_4	115.3	121.3	134.7[c]

[a] kcal mol^{-1}. [b] Ref. 25. [c] Ref. 26.

MP2/6-31G* calculations seem to indicate that no intermediate exists between $C_2H_7^+ \cdot FH$ and the products.

The structure of the transition state and the intermediate obtained in the 6-31G* calculation are represented in Figure 4. The Mulliken population analysis for both structures indicates that the net charge over the H_2F fragment is 0.739 au at the transition state and 0.794 au at the intermediate. These charges and the values of the interatomic distances allow us to describe these structures as $C_2H_6 \cdot H_2F^+$ complexes, the only appreciable difference being the degree of proton transfer reached. The fact that the $C_2H_6 \cdot H_2F^+$ intermediate is less stable than $C_2H_7^+ \cdot FH$ can be understood in terms of the difference in proton affinity between ethane and hydrogen fluoride. In Table 6 the calculated

Table 7. Dissociation energy[a] of the $C_2H_7^+ \cdot FH$ intermediate into $C_2H_7^+$ and HF.

Level of calculation	E
3-21G	15.4
6-31G*	10.8
MP2/6-31G*[b]	13.7

[a] kcal mol^{-1}. [b] At the 6-31G* geometry.

and experimental values of these proton affinities are presented. The results obtained with both basis sets are in good agreement with the experimental values. The proton affinity of ethane is notably greater than that of hydrogen fluoride, the $C_2H_7^+ \cdot FH$ intermediate being thus more stable.

As shown in Scheme 2, another possible process that leads to the formation of ethane is the dissociation of the $C_2H_7^+ \cdot FH$ intermediate (pathway B). We present in Table 7 the computed dissociation energy of $C_2H_7^+ \cdot FH$ into $C_2H_7^+$ and HF. At all levels of calculation this energy is much lower than the energy associated with the proton-transfer process discussed in the preceding paragraph.

After dissociation, $C_2H_7^+$ must lose a proton to yield ethane. In the gas phase this deprotonation can take place in the presence of HF or CH_3F, which act as bases. Given that methyl fluoride has a greater proton affinity than hydrogen fluoride (see above), the proton transfer to methyl fluoride seems to be more favourable. The energy associated with this process is -9.3 kcal mol^{-1} at the 6-31G* level, while the value corresponding to the proton transfer to HF is 19.8 kcal mol^{-1} at the same level of calculation.

The results obtained from a study of the electrophilic attack step show that the mechanism which is energetically most favourable is that represented in Scheme 2, in which protonated methyl fluoride attacks methane to yield a $C_2H_7^+ \cdot FH$ intermediate. This complex dissociates, according to path B, into $C_2H_7^+$ and HF. Finally this $C_2H_7^+$ carbocation transfers its proton to a new methyl fluoride molecule. The mechanism of the whole process is represented in Scheme 3.

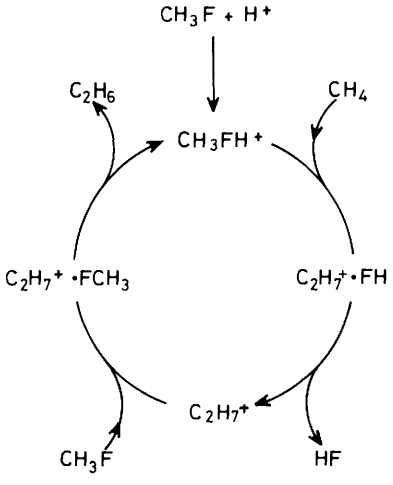

Scheme 3.

Comparison with the $CH_4 + H_2F^+$ *Reaction.*—Let us now compare the results presented in this paper with those corresponding to the reaction of methane with hydrogen fluoride, catalysed by H^+, which have been already published.[15] Since our previous study was performed using the 3-21G basis set, we will consider in this section only the results obtained with this basis set.

In the reaction of methane with CH_3FH^+ we have found a $C_2H_7^+ \cdot FH$ structure which corresponds to an energy minimum, this result being in good agreement with the mechanism proposed by Olah *et al.*[5] In the reaction of methane with H_2F^+ an analogous structure, $CH_5^+ \cdot FH$, has also been found.[15] However, this structure does not correspond to an energy minimum but to a transition state. This striking difference between the results of both reactions can be understood if we take into account the calculated proton affinities of methane, ethane, and hydrogen fluoride presented in Table 6.

One can observe that ethane has a greater proton affinity than methane, the theoretical results being in good agreement with this fact. As regards hydrogen fluoride, its experimental proton affinity is lower than that of methane and ethane. However, the 3-21G calculation does not agree with this result and gives a proton affinity for hydrogen fluoride notably greater than that of methane. This overestimation of the proton affinity of HF seems to be the reason for which no stable $CH_5^+ \cdot FH$ intermediate appears in the 3-21G calculation.

With the 6-31G* basis set there is also a discrepancy between the experimental ordering of proton affinities, but in this case the difference between the computed proton affinities of methane and hydrogen fluoride is much lower. Therefore, one could expect the presence of a $CH_5^+ \cdot FH$ intermediate in the 6-31G* potential hypersurface. This possibility has been confirmed and the intermediate has been localized, its formation energy from CH_4 and H_2F^+ being -15.6 kcal mol^{-1} and its dissociation energy into CH_5^+ and HF being 16.6 kcal mol^{-1}.

Conclusions

In this work we have studied the Friedel–Crafts alkylation reaction of methyl fluoride with methane, uncatalysed and catalysed by H^+. We have found that the uncatalysed reaction presents a very great energy barrier. The catalyst notably increases the reaction rate by increasing the electrophilic character of the alkylating agent, in this case methyl fluoride. The catalysed reaction takes place through a multistep process with different alternative paths. The most favourable path seems to be that which involves formation of a $C_2H_7^+ \cdot FH$ complex which subsequently dissociates, yielding the $C_2H_7^+$ carbocation.

The use of such an extreme example of acid catalyst, such as H^+, leads us to think that the catalytic effect we have obtained in our calculations is overestimated by comparison with that which would correspond to more realistic catalysts. Furthermore, our calculations have simulated the process in the gas phase; the results may be different in solution, due to the presence of charged structures. In spite of these limitations, our results allow an insight into the general trends of acid catalysis in Friedel–Crafts reactions.

References

1 G. A. Olah, 'Friedel–Crafts Chemistry,' Wiley, New York, 1975.
2 J. D. Heldmann, *J. Am. Chem. Soc.*, 1944, **66**, 1791.
3 L. Schmerling, *J. Am. Chem. Soc.*, 1949, **71**, 701.
4 G. A. Olah, S. Kuhn, and J. Olah, *J. Chem. Soc.*, 1957, 2174.
5 G. A. Olah, G. Klopman, and H. Schosberg, *J. Am. Chem. Soc.*, 1969, **91**, 3261.
6 H. Mayr and W. Strieppe, *J. Org. Chem.*, 1983, **48**, 1159.
7 H. M. Nelson, *J. Phys. Chem.*, 1962, **66**, 1380.
8 R. Nakane, O. Kurihara, and A. Natsubori, *J. Phys. Chem.*, 1964, **68**, 2876.
9 R. Nakane, A. Natsubori, and O. Kurihara, *J. Am. Chem. Soc.*, 1965, **87**, 3597.
10 G. A. Olah, J. DeMember, R. H. Schosberg, and Y. Halpern, *J. Am. Chem. Soc.*, 1972, **94**, 156.
11 E. Silla, E. Scrocco, and J. Tomasi, *Theor. Chim. Acta*, 1975, **40**, 343.
12 G. Alagona, E. Scrocco, E. Silla, and J. Tomasi, *Theor. Chim. Acta*, 1977, **45**, 127.

13 W. L. Jorgensen and M. E. Cournoyer, *J. Am. Chem. Soc.*, 1978, **100**, 5278.
14 J. Bertrán, F. Mora, and E. Silla, *J. Chem. Soc., Perkin Trans. 2*, 1982, 647.
15 V. Branchadell, A. Oliva, and J. Bertrán, *J. Mol. Catal.*, 1988, **44**, 285.
16 GAUSSIAN-86, M. J. Frisch, J. S. Binkley, H. B. Schlegel, K. Raghavachari, C. F. Melius, R. L. Martin, J. J. P. Stewart, F. W. Brobrowicz, C. M. Rohlfing, L. R. Kahn, D. J. DeFrees, R. Seeger, R. A. Whiteside, D. J. Fox, E. M. Fleuder, and J. A. Pople, Carnegie-Mellon Quantum Chemistry Publishing Unit, Pittsburg, PA, USA, 1984.
17 J. S. Binkley, J. A. Pople, and W. J. Hehre, *J. Am. Chem. Soc.*, 1980, **102**, 939.
18 P. C. Hariharan and J. A. Pople, *Theor. Chim. Acta*, 1973, **28**, 213.
19 (*a*) C. Møller and M. S. Plesset, *Phys. Rev.*, 1934, **34**, 618; (*b*) J. S. Binkley and J. A. Pople, *Int. J. Quantum Chem.*, 1975, **9**, 229.
20 H. B. Schlegel, *J. Comput. Chem.*, 1982, **3**, 214.
21 J. A. Pople, H. Krishnan, H. B. Schlegel, and J. S. Binkley, *Int. J. Quantum Chem., Symp.*, 1979, **13**, 225.
22 J. L. Beauchamp, D. Holtz, S. D. Woodgate, and S. L. Patt, *J. Am. Chem. Soc.*, 1972, **94**, 2798.
23 K. Hiraoka and P. Kebarle, *J. Am. Chem. Soc.*, 1976, **98**, 6119.
24 K. Raghavachari, R. A. Whiteside, J. A. Pople, and P. v. R. Schleyer, *J. Am. Chem. Soc.*, 1981, **103**, 5649.
25 M. S. Forster and L. J. Beauchamp, *Inorg. Chem.*, 1975, **14**, 1229.
26 T. B. McMahon and P. Kebarle, *J. Am. Chem. Soc.*, 1985, **107**, 2612.

Received 27*th* October 1988; *Paper* 8/04289F